Analysis of a topographic-based InSAR SWE estimation technique for low-land permafrost terrain north of Inuvik, Northwest Territories

Allison Plourde

Department of Engineering Science, Simon Fraser University, Burnaby, British Columbia, Canada

ABSTRACT

InSAR (Interferometric Synthetic Aperture Radar) is a well-established method for measuring small-scale surface deformations over large regions; however, contaminating effects of snow cover on the InSAR phase prevents the use of (usually less noisy) winter InSAR data, limiting the accuracy of comprehensive measurement of seasonal dynamics in permafrost terrain. In this study we investigate if a previously developed topography-based approach for estimating the contribution of the Snow Water Equivalent (SWE) from repeat pass InSAR phase is accurate enough to correct the displacement phase of the winter data. We use a stack of TerraSAR-X strip map data covering several winters over a study region located in low-lying permafrost north of Inuvik, Northwest Territories. In the study region several ground truth sites have been instrumented with (1) an inclinometer to measure vertical surface deformation due to active layer dynamics of the permafrost, and (2) an ultra-sonic range finder to measure snow-depth. Our analysis found a high uncertainty in the topographic SWE estimates around our ground truth sites due to insufficient variation in terrain preventing us from evaluating the method directly against the ground truth. Estimates for other areas with higher terrain variability farther away from our ground truth sites, however, showed more promising results in terms of error estimates from the topographic SWE estimation being small enough to correct the phase of winter InSAR data to allow their use for comprehensive permafrost active layer displacement measurements.

1 INTRODUCTION

Differential Interferometric Synthetic Aperture Radar (DInSAR) is an established method for precise measurement of surface deformations across large expanses. In terrain underlain by permafrost, the seasonal freeze-thaw cycle can result in widespread surface deformations on the order of millimeters to centimeters, making it appropriate for measurement using InSAR techniques (Liu et al. 2010, 2014; Short et al. 2011). The active layer of permafrost refers to the upper portion of the ground that experiences seasonal freezing and thawing. During freeze back, moisture in the active layer freezes. When the excess water freezes, it undergoes an increase in volume; the expansion exerts pressure on the surrounding soil, causing the ground to heave. Alongside seasonal deformations, long-term subsidence trends stemming from permafrost degradation are also of concern. Distinguishing the seasonal signal from long-term trends is necessary for certain applications, such as estimating Active Layer Thickness (ALT; Liu et al. 2012; Schaefer et al. 2015). Separating these signals can be difficult due to decorrelation of the InSAR phase during spring, when snow is melting, as well as in the fall when snow begins to accumulate; hence, InSAR analyses are often limited to snow-free scenes (Liu et al. 2010, 2014; Short et al. 2011; Strozzi et al. 2018; Rouyet et al. 2019; Scheer et al. 2023).

Phase coherence in InSAR refers to the stability and consistency of the phase measurements over time. Phase decorrelation occurs due to alterations in surface characteristics, such as variations in soil moisture, vegetation, and snow cover on the scale of the microwave wavelength (in these media). In the case of cold, dry snow, the snow layer also acts as a refracting medium. While interferometric pairs with and without snow may exhibit complete decorrelation, pairs captured with short time intervals during the dry-snow season can demonstrate high coherence (Guneriussen et al. 2001). Additionally, after freeze back, the ground surface is relatively stable; thus, if the phase due to snow could be accounted for, long-term trends independent of the seasonal freeze-thaw cycle could be established using winter scenes.

Furthermore, an increase in mean annual snow cover can increase ground temperatures and deepen the active layer, causing the ground to gradually subside from thaw of ice-rich permafrost (Burn et al. 2009). Consequently, there is a need for the ability to accurately monitor snow cover over large areas for which InSAR techniques, such as the method examined in this paper, could prove to be a viable solution.

In this paper, the suitability of a topographic-based approach for estimating the Snow Water Equivalent (SWE) with InSAR (Eppler et al. 2022) to correct the phase of winter InSAR data (so that only the displacement phase component remains) is evaluated for a region of low-land, continuous permafrost in a tundra environment north of Inuvik, Northwest Territories. Section 2 provides background on the relevant InSAR techniques for snow-covered and permafrost landscapes followed by a description of the research area in Section 3. Section 4 outlines the methodology used for both in situ field measurements as well as the InSAR processing steps. In Section 5, the results are presented followed by a discussion in Section 6.

2 BACKGROUND

Repeat pass InSAR (DInSAR) is a remote sensing technique that can measure mm-scale displacements by measuring the phase difference between two synthetic aperture radar (SAR) acquisitions taken at different times. Radar satellites have the advantage of providing a cost-

https://doi.org/10.52381/ICOP2024.65.1

effective solution of monitoring large regions of land over many years.

In general, the interferometric phase, ϕ, is a result of the superposition of several components (Equation 1).

$$\phi_{total} = \phi_{topographic} + \phi_{atmospheric} + \phi_{soil\ moisture} + \phi_{snow} + \phi_{surface\ displacement} \quad [1]$$

The challenge of InSAR measurements is separating these components to isolate the desired element, such as surface displacement. Studies that have measured permafrost-related surface displacements using InSAR methods have often limited the analysis to snow-free scenes due to the complexities introduced by the presence of snow (Liu et al. 2010, 2014; Short et al. 2011; Strozzi et al. 2018; Rouyet et al. 2019; Scheer et al. 2023). However, snow cover is often present throughout a significant portion of the year in regions with continuous permafrost; thus, eliminating such scenes can significantly reduce the amount of available data.

Several approaches have emerged to measure SWE from both SAR and InSAR scenes. SAR methods use principles of backscatter — the amplitude of the SAR signal — to measure SWE (Tsang et al. 2022), whereas InSAR methods examine the phase difference between two SAR acquisitions. When considering the effect of snow on the InSAR signal, there are two mechanisms that need to be considered. Firstly, radar signals are impenetrable to liquid water, hence when snow is wet (during thaw) the signal is reflected at the snow surface. Methods that have capitalized on this mechanism compare snow-free and wet snow scenes to measure total SWE (Larsen et al. 2005). When snow is dry, the signal is reflected at the snow-ground interface resulting in a signal delay due to refraction in the snow-layer (Guneriussen et al. 2001). Methods that take advantage of this mechanism include the delta-k method (Engen et al. 2004), the method in this paper which exploits variations in topography (Eppler et al. 2022), among others (Guneriussen et al. 2001; Leinss et al. 2015; Lei et al. 2016).

3 Ground Truth Sites

The study area is situated in low-lying permafrost terrain north of Inuvik, Northwest Territories in the uplands of the Mackenzie Delta (Figure 1). Several ground truth sites have been established where in situ measurements of vertical surface displacement along with snow depth are collected year-round.

The ground truth sites are located between kilometer 20 and 35 of the Inuvik-Tuktoyaktuk Highway (ITH) within 400 m of the road. The study uses satellite images from TerraSAR-X, the footprint covers a 13 km by 30 km area extending from the west side of Noell lake up to just south of Trail Valley Creek.

The research area is part of the continuous permafrost zone and is characterized by low-shrub tundra. The surficial geology is predominantly hummocky and rolling moraine, interspaced by colluvial and lacustrine deposits (Rampton

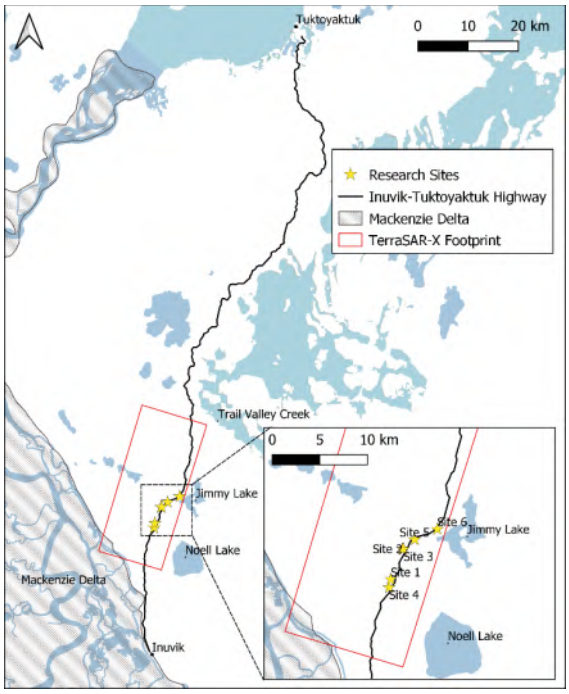

Figure 1. Overview of study Area. Depicted are the six ground truth sites with instrumentation for in situ measurements as well as the footprint for the TerraSAR-X strip map radar stack.

1987). Ground temperatures in the uplands decrease northwards across the treeline, and the thickness of snow cover also decreases in this direction (Burn and Kokelj 2009).

3.1 Detailed Site Description

Homogenous Terrain (Sites 1 and 4): Site 1 was established in 2018 and is the longest running site, covering a 4-year record of inclinometer measurements along with a 3-year record of snow depth measurements. Site 4 was established in 2022 with inclinometer measurements for that year. Regions of polygonal wedges surround these sites and permafrost related activity, such as frost boils are visible within the vicinity. Site 1 has been determined to be underlain by ice-rich permafrost, whereas site 4 was discovered not to be ice-rich.

Undulating Terrain (Sites 2 and 3): Site 2 and 3 were established in 2019 and due to instrumentation errors have sparse data. Undulating terrain was desirable to determine if the topographical approach for InSAR SWE estimation would be suitable for this area.

Sloping Lacustrine Terrain (Sites 5 and 6): Sites 5 and 6 were established in 2022 and both contain inclinometer and snow depth measurements dating from July 2022 to July 2023. They were selected for their proximity to sloping terrain as well as coherence in the InSAR imagery in both summer and winter months.

4 METHODOLOGY

Using a collection of TerraSAR-X strip map images, we evaluate the viability for DInSAR phase correction of a method developed by Eppler et al. (2022) that exploits variations in topography to quantify the effects of SWE on interferometric phase. By identifying the phase component due to SWE, an avenue is established for the measurement of surface deformation throughout the winter season.

The method exploits variations in topographic slope according to Equation 2.

$$\xi \doteq \frac{d\Phi_{SWE}}{dSWE} = \frac{4\pi}{\lambda\rho}\cos\alpha\left(\sqrt{\epsilon(\rho) - \sin^2\theta} - \cos\theta\right) \quad [2]$$

Where ξ is the sensitivity and is defined as the change in phase due to SWE, Φ_s, versus the change in SWE itself. This component is dependent on the radar wavelength, λ, the density of the snow ρ, the terrain slope angle, α, the permittivity of snow ϵ, and the local incidence angle θ. The snow density is assumed to be 0.3, a suitable assumption according to previous studies (Leinss et al. 2015; Eppler et al. 2022). Considering that the method estimates the relative change in SWE rather than total SWE, ρ is also related to changes in the snowpack rather the absolute ρ. In Eppler 2022, it was shown that misspecification of ρ for values between 0 and 0.5 would result in a positive or negative bias of less than 5% the total SWE. The permittivity is derived from ρ according to Leinss et al. (2015). The wavelength and incidence angle are known values of the satellite configuration and the slope angle can be derived from a Digital Elevation Model (DEM).

The ground truth sites are equipped with inclinometers to measure vertical deformation and ultrasonic range finders to measure snow depth (Figure 2).

Figure 2. (A) Ultrasonic snow depth sensor and (B) inclinometer. The center pole is mounted into the permafrost such that it remains stationary.

4.1 Inclinometer Measurements

The vertical surface displacement is derived from the inclination angle measured by either an RST tilt logger or GeoPrecision tilt logger attached to a lever arm. The mechanism design is based on Gruber (2020). A sample of vertical surface displacement recorded between July 2022 and July 2023 at each of the sites is provided in Figure 3.

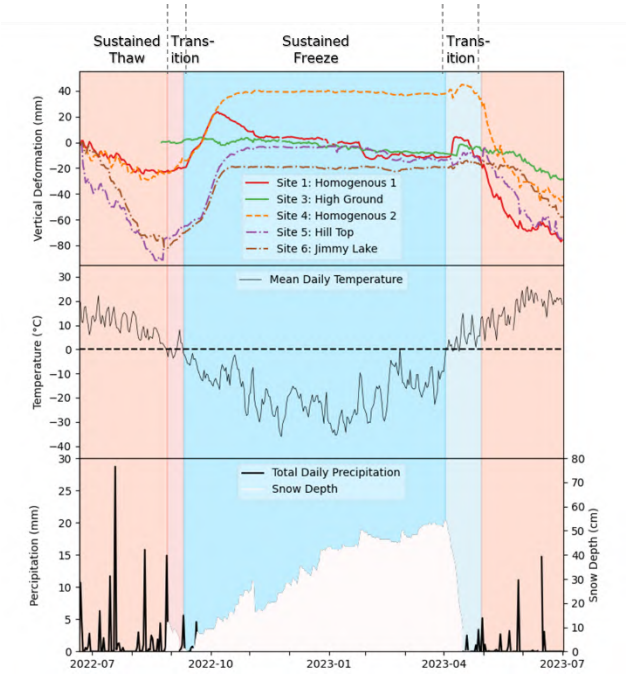

Figure 3. (Top) Vertical deformation as measured by inclinometers between July 2022 and July 2023. (Middle) Mean daily temperature and (bottom) precipitation at Inuvik (Environment Canada).

From the inclinometer data, it can be observed that there is marginal surface displacement from the beginning of November through to the end of March, with the exception of site 1, which recorded a downward trend in subsidence throughout the winter. The mechanism of this downward trend is unclear and may be due to errors related to the weight of snow accumulation or in the sensor setup itself; however, there are mechanisms that can result in negative heave (Mackay et al. 1979). For simplicity, and due to the overall similarities between sites 1 and 4, it was assumed for this analysis that this phenomenon was isolated, and that for the spatial scale of the SWE estimates in this analysis, heave between November and March could be neglected. These measurements, as described in the next section, are used in this study to correct the snow depth measurements for surface heave.

4.2 Snow Depth Measurements

The snow depth was measured at five sites using a Judd ultra sonic sensor designed for snow depth measurements. Sites 1–3 were instrumented with sensors in 2019, sites 5–6 were installed in 2022. Snow depth at each of the sites for

the 2022–2023 season is shown in Figure 4. Site 4 was instrumented with an experimental sensor that did not hold up in the harsh conditions of the tundra and so no data are available at this site.

Two corrections need to be applied to the snow depth data. Firstly, to avoid spurious measurements of vegetation height, the date of first snow at Inuvik is used to zero the data. Additionally, as can be seen in Figure 2A, the pole supporting the sensor is anchored into the permafrost, thus, the ground is free to move and the sensor would also be subject to detecting changes in the ground height due to heave and subsidence. As shown in Figure 3 these displacements can be quite significant. The tilt logger data was used to correct for these displacements; a sample of the 'heave-corrected' snow depths for the 2022–2023 season are provided in Figure 4 along with Environment Canada data collected at Inuvik and Trail Valley climate stations. Inclinometer data at site 2 was not available and was not included.

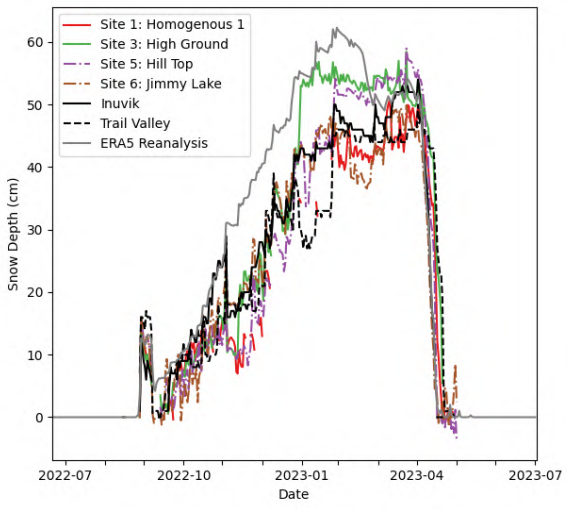

Figure 4. (Top) Heave-Corrected in situ snow depth measurements for 2022-2023 alongside measurements from the Inuvik and Trail Valley Environment Canada climate stations.

5 InSAR Processing

A stack of 106 TerraSAR-X strip map scenes were collected spanning from February 2018 until August 2023. Of those, a total of 78 pairs could be formed that had a 11-day interval between the time of acquisition, 30 of which were between the months of November through to the end of March where snowfall would be present and surface heave would be negligible. The interferograms were generated using standard processing steps using the GAMMA software package (GAMMA Remote Sensing AG, Switzerland).

Firstly, the single-look complex (SLC) scenes were registered to a common master scene and multi-looked by a factor of 2 in both range in azimuth. They were topographically corrected with a Tandem-X 12m DEM. Adaptive phase filtering was then applied using a Werner-Goldstein filter.

For this analysis, atmospheric effects on the InSAR phase are mitigated by estimating the SWE in 1 km^2 windows, such that the dynamic atmosphere is assumed to be constant. Finally, the SWE estimation method does not require phase unwrapping, in which the 2π ambiguity of the InSAR data is resolved (Eppler et al. 2022).

6 Results

The SWE was estimated for 30 interferograms and compared to in situ data collected at the sites, Environment Canada climate data for the Inuvik and Trail Valley stations, as well as ERA5 reanalysis data.

A sensitivity map for the study area based on Equation 2 is shown in Figure 5. The SWE estimation method is dependent on the local spatial variability in the phase sensitivity. The standard deviation over 1 km^2 windows was calculated for the de-meaned 2D sensitivity map to estimate the quality of SWE estimations in Figure 5. It can be observed that much of the region, which is dominated by relatively flat terrain, has a low standard deviation in ξ. The areas where there is the highest standard deviation are deep cut valleys in the terrain as shown in Figure 6.

In addition to variability in SWE, the magnitude of the local incidence angle may also be of concern in producing accurate results since steeper angles result in smaller changes in path-length of the signal through dry snow. The relationship between incidence angle and phase due to 10 mm of SWE over a constant slope is shown in Figure 7. It can be observed for steep incidence angles, there is very little change in phase; between 0 and 25°, with respect to the local terrain slope, the phase varies by 0.26 rad for 10 mm of SWE. For angles above 25° the difference in phase due to the local incidence angle becomes much more pronounced; between 25° and 50°, the phase varies by 1.71 rad. It was discovered that a sufficiently shallow incidence angle with respect to the local slope of the terrain was required to get precise estimations since shallower angles increase the modulating effect of SWE on the phase, which the algorithm is dependent on; thus, a thresholding mask was used to limit the estimation to areas where α was greater than 25°, the result of which is also shown in Figure 6.

It can be observed that the ground truth sites set up in this study are in a region of low variability in terrain slope and thus, low sensitivity to the SWE estimation method. For this reason, an additional point in the region of highest variability in sensitivity was also included in the SWE estimation results. The SWE for each point is taken to be the average over a circular region around the point with a diameter of roughly 300 m – which corresponds to an average over about 2000 pixels. This point is compared to the SWE at Inuvik in Figure 8. The color of the points in the figure represents the mean coherence of the area and the error bars represent the standard deviation of the estimated SWE in the area. Results for SWE estimations at site 1 compared with the in situ data are shown in Figure 9.

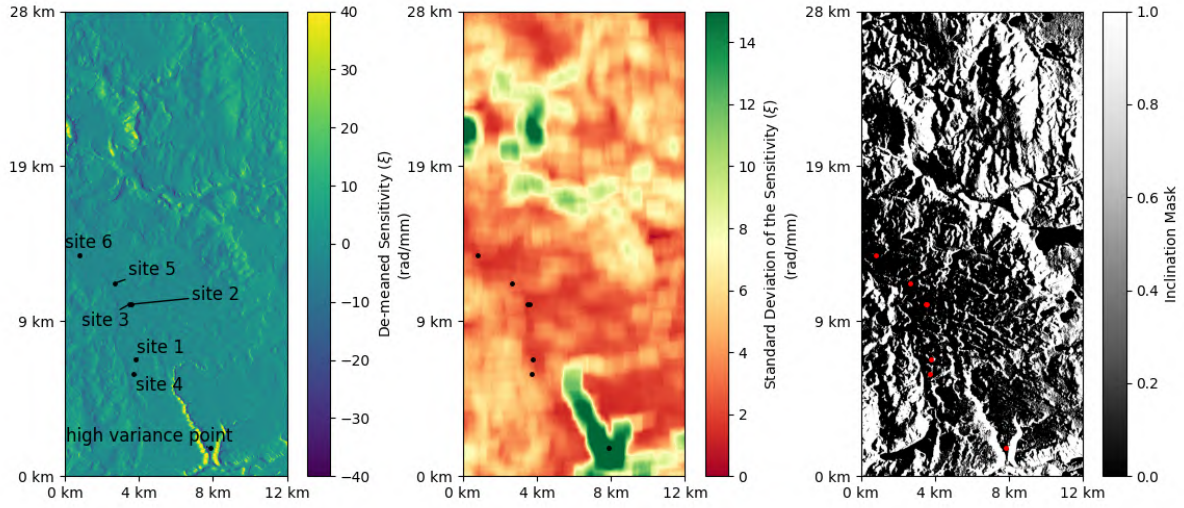

Figure 5. (Left) Derived sensitivity map with ground truth sites indicated. (Middle) A ξ quality map derived from the standard deviation of the sensitivity map. Areas in green indicate regions with high variability in ξ and thus are expected to provide quality estimations for SWE. (Right) Local incidence angle masking used to eliminate regions with a steep incidence angle (black) from the SWE estimation.

Figure 6. Example of terrain with a high variability of sensitivity to SWE north of site 6.

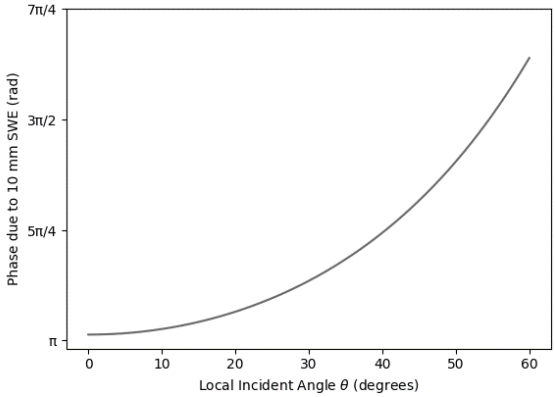

Figure 7. Resulting phase component due to 10 mm of SWE over constant sloped terrain with varying local incidence angle according to Equation 2.

The in situ data are compared to the coarser ERA5 Reanlysis data in Figure 10. Comparing the in situ data provides insight into the spatial variability of the SWE and the expected error when comparing the InSAR results to the in situ measurements. Excluding sites 5 and 6, where minimal data are available, the average Root Mean Squared Error (RMSE) between the in situ data and ERA5 data is 18.6 mm of SWE. The InSAR estimate for the region with high variability in ξ showed a similar RMSE compared to the Inuvik data, which was the closest in situ measurement, of 15.8 mm of SWE. The RMSE between the InSAR estimate for site 1 compared with the in situ measurement at site 1 was much higher, with a value of 38.8 mm of SWE.

7 Discussion

The objective of this analysis was to assess the applicability of a topographic-based InSAR method for estimating Snow Water Equivalent (SWE). The motivation behind this investigation was to assess the potential for the method to account for the phase due to snow, enabling the measurement of long-term subsidence trends using winter InSAR data. The SWE estimations were limited to the period between November and March in which the inclinometer data showed that there would be negligible surface movement.

In situ snow depth was measured at 4 of the 6 ground truth sites as well as Inuvik and Trail Valley Environment Canada stations and compared to the coarser ERA5 Reanalysis data. These measurements were converted to SWE by assuming a snow density of 0.3. The variability of the in situ data was found to be similar to the variability in the InSAR estimates at the point with high variability in ξ, suggesting that the method may be suitable for this particular region.

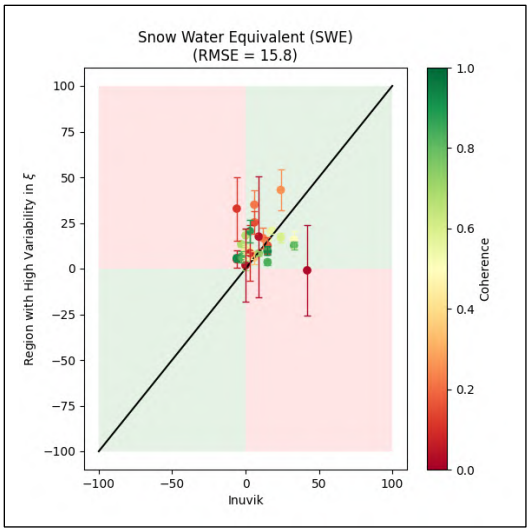

Figure 8. Estimated SWE at location with high variation in ξ compared with derived SWE from measured snow depth at Inuvik. The coherence of the window is indicated by color and the error bars represent the standard deviation of the SWE estimation.

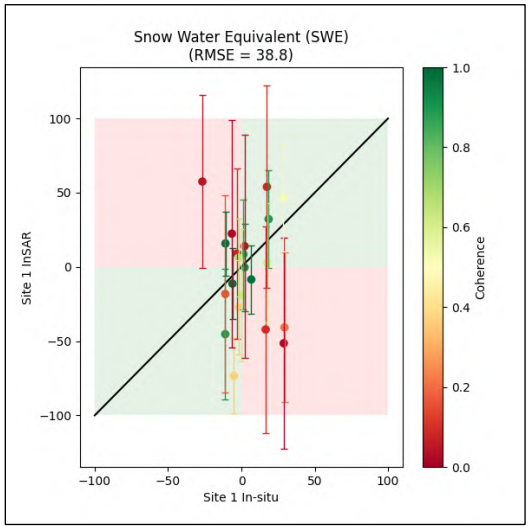

Figure 9. Estimated SWE at site 1 compared with in situ measurements. Due to the low variability in ξ in this region, there is a greater uncertainty in the results.

However, there was substantially more variability between the InSAR estimates for site 1 when compared to the site 1 in situ measurements.

In the region with high variability in ξ, the InSAR estimates tended to be higher than values reported at Inuvik and Trail Valley. However, this area is a region of deep cut valleys and so may be more prone to snow accumulation, resulting in the higher estimates.

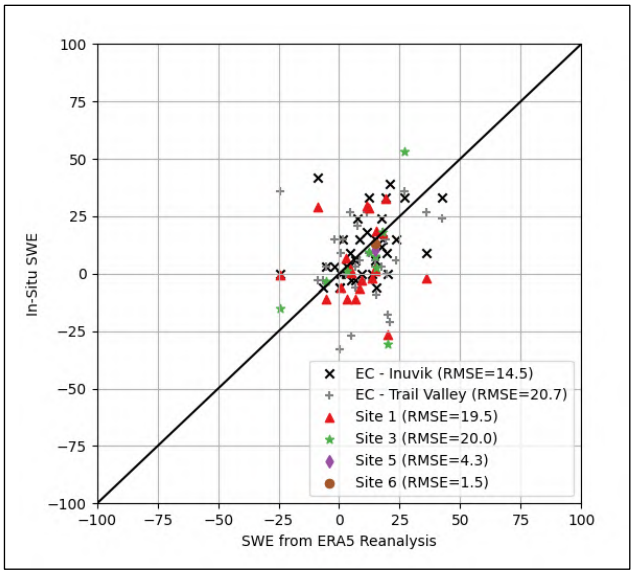

Figure 10. Relative in situ SWE compared with coarse ERA5 Reanalysis data.

The ground truth sites were located in a region with low variability in ξ. There was a high standard deviation, resulting in a greater uncertainty in the predictions at the ground truth sites when compared to the region with high variability. For this reason, along with the higher RMSE, it is believed that the SWE estimation method detailed here in this report may not be suitable for such regions. However, the estimation method showed more promising results at these sites when the area in the interferograms had a higher coherence.

Using the in situ data, it may be possible to derive a phase based on the snow depth measurements according to Equation 2. When averaged over large spatial areas, such phase screens could be used to correct the InSAR stack for the phase component due to snow. Established DInSAR techniques could then be applied to the corrected interferograms, thus, allowing for measurement of surface displacement in winter months.

The steep incidence angle of the TerraSAR-X strip map imaging mode used in this study may be a limiting factor to the applicability of this method. In the future, it would be useful to perform similar studies with a shallower incidence angle. Additionally, in situ ground truth stations setup in the regions with high variability in ξ would be beneficial to further validate the SWE estimation method. The largest limiting factor in this study was the low variability in the terrain at the in situ ground truth sites.

8 CONCLUSIONS

This paper investigated the use of a previously established method (Eppler et al. 2022) for estimating the snow water equivalent (SWE) over large areas using InSAR. The method exploits variations in topographic slope to estimate the SWE. It was discovered that this method may not be suitable for correcting winter InSAR phase for areas with low variability in topography. Additionally, it was also

presumed that the incidence angle of the radar sensor may also be important to consider, noting that the incidence angle of the TerraSAR-X strip map stack of roughly 24° is too steep to generate the variation in sensitivity required to detect changes in SWE precisely as the algorithm relies on the modulating effect SWE has on the phase; there is a greater modulating effect for shallower angles as the path of the signal travels a greater distance through the snow layer.

The data was compared to in situ snow depth data that was corrected for surface heave due to freeze back. However, due to the low variation in terrain slope and sparse availability of suitable interferometric pairs, a robust comparison between the in situ and InSAR data unfortunately could not be obtained. We discovered that the in situ data, when corrected for heave, was representative of the data obtained at nearby Environment Canada climate stations and so such datasets should be useful therefore for studying the effectiveness of the SWE retrieval algorithm in areas of higher terrain variability where SWE errors are smaller.

9 ACKNOWLEDGEMENTS

We extend our gratitude to the Permafrost Network and the Geological Survey of Canada's Climate Change Geoscience Program for their invaluable support and funding, which were instrumental in making our research endeavors possible.

Special thanks are also due to Peter Morse and H. Brendan O'Neill for their exceptional assistance and guidance in the field. Their expertise greatly enhanced the quality of our work.

10 REFERENCES

Burn, C.R. and Kokelj, S.V. 2009. 'The environment and permafrost of the Mackenzie Delta area', *Permafrost and Periglacial Processes* 20, pp. 83–105. Available at: https://doi.org/10.1002/ppp.655.

Burn, C.R., Mackay, J.R., and Kokelj, S.V. 2009. 'The thermal regime of permafrost and its susceptibility to degradation in upland terrain near Inuvik, N.W.T.', *Permafrost and Periglacial Processes* 20, pp. 221–227. Available at: https://doi.org/10.1002/ppp.649.

Engen, G., Guneriussen, T., and Overrein, Y. 2004. 'Delta-K interferometric SAR technique for snow water equivalent (SWE) retrieval', *IEEE Geoscience and Remote Sensing Letters* 1, pp. 57–61. Available at: https://doi.org/10.1109/LGRS.2003.822880.

Eppler, J., Rabus, B., and Morse, P. 2022. 'Snow water equivalent change mapping from slope-correlated synthetic aperture radar interferometry (InSAR) phase variations', *The Cryosphere* 16, pp. 1497–1521. Available at: https://doi.org/10.5194/tc-16-1497-2022.

Guneriussen, T., Hogda, K.A., Johnsen, H., and Lauknes, I. 2001. 'InSAR for estimation of changes in snow water equivalent of dry snow', *IEEE Transactions on Geoscience and Remote Sensing* 39, pp. 2101–2108. Available at: https://doi.org/10.1109/36.957273.

Gruber, S. 2020. 'Ground subsidence and heave over permafrost: hourly time series reveal interannual, seasonal and shorter-term movement caused by freezing, thawing and water movement', *The Cryosphere* 14, pp. 1437–1447. Available at: https://doi.org/10.5194/tc-14-1437-2020.

Larsen, Y., Malnes, E., and Engen, G. 2005. 'Retrieval of snow water equivalent with envisat ASAR in a norwegian hydropower catchment', in *IEEE International Geoscience and Remote Sensing Symposium*, 2005. Seoul, South Korea: pp. 5444–5447. Available at: https://doi.org/10.1109/IGARSS.2005.1525972.

Lei, Y., Siqueira, P., and Treuhaft, R. 2016. 'A dense medium electromagnetic scattering model for the InSAR correlation of snow', *Radio Science* 51, pp. 461–480. Available at: https://doi.org/10.1002/2015RS005926.

Leinss, S., Wiesmann, A., Lemmetyinen, J., and Hajnsek, I. 2015. 'Snow Water Equivalent of Dry Snow Measured by Differential Interferometry', *Journal of Selected Topics in Applied Earth Observations and Remote Sensing* 8, pp. 3773–3790. Available at: https://doi.org/10.1109/JSTARS.2015.2432031.

Liu, L., Zhang, T., and Wahr, J. 2010. 'InSAR measurements of surface deformation over permafrost on the North Slope of Alaska', *Journal of Geophysical Research: Earth Surface* 115. Available at: https://doi.org/10.1029/2009JF001547.

Liu, L., Schaefer, K., Zhang, T., and Wahr, J. 2012. 'Estimating 1992–2000 average active layer thickness on the Alaskan North Slope from remotely sensed surface subsidence', *Journal of Geophysical Research: Earth Surface* 117. Available at: https://doi.org/10.1029/2011JF002041.

Liu, L., Jafarov, E.E., Schaefer, K.M., Jones, B.M., Zebker, H.A., Williams, C.A., Rogan, J., and Zhang, T. 2014. 'InSAR detects increase in surface subsidence caused by an Arctic tundra fire', *Geophysical Research Letters* 41, pp. 3906–3913. Available at: https://doi.org/10.1002/2014GL060533.

Mackay, J.R., Ostrick, J., Lewis, C.P., and Mackay, D.K. 1979. 'Frost Heave at Ground Temperatures Below Zero Degrees Centigrade, Inuvik, Northwest Territories', *Geological Survey of Canada* Current Research Part A, pp. 403–406. doi:10.4095/104879.

Rampton, V.N. 1987. 'Surficial Geology, Tuktoyaktuk Coastlands, District of Mackenzie, Northwest Territories', *Geological Survey of Canada* "A" Series Map 1647A, 1 sheet. Available at: https://doi.org/10.4095/125160.

Rouyet, L., Lauknes, T.R., Christiansen, H.H., Strand, S.M., and Larsen, Y. 2019. 'Seasonal dynamics of a permafrost landscape, Adventdalen, Svalbard, investigated by InSAR', *Remote Sensing of Environment* 231, 111236. Available at: https://doi.org/10.1016/j.rse.2019.111236.

Schaefer, K., Liu, L., Parsekian, A., Jafarov, E., Chen, A., Zhang, T., Gusmeroli, A., Panda, S., Zebker, H.A., and Schaefer, T. 2015. 'Remotely Sensed Active Layer Thickness (ReSALT) at Barrow, Alaska Using Interferometric Synthetic Aperture Radar', *Remote Sensing* 7, pp. 3735–3759. Available at: https://doi.org/10.3390/rs70403735.

Scheer, J., Caduff, R., How, P., Marcer, M., Strozzi, T., Bartsch, A., and Ingeman-Nielsen, T. 2023. 'Thaw-Season InSAR Surface Displacements and Frost Susceptibility Mapping to Support Community-Scale Planning in Ilulissat, West Greenland', *Remote Sensing* 15, 3310. Available at: https://doi.org/10.3390/rs15133310.

Short, N., Brisco, B., Couture, N., Pollard, W., Murnaghan, K., and Budkewitsch, P. 2011. 'A comparison of TerraSAR-X, RADARSAT-2 and ALOS-PALSAR interferometry for monitoring permafrost environments, case study from Herschel Island, Canada', *Remote Sensing of Environment* 115, pp. 3491–3506. Available at: https://doi.org/10.1016/j.rse.2011.08.012.

Strozzi, T., Antonova, S., Günther, F., Mätzler, E., Vieira, G., Wegmüller, U., Westermann, S., and Bartsch, A. 2018. 'Sentinel-1 SAR Interferometry for Surface Deformation Monitoring in Low-Land Permafrost Areas', *Remote Sensing* 10, 1360. Available at: https://doi.org/10.3390/rs10091360.

Tsang, L., Durand, M., Derksen, C., Barros, A.P., Kang, D.-H., Lievens, H., et al.2022. 'Review article: Global monitoring of snow water equivalent using high-frequency radar remote sensing', *The Cryosphere* 16, pp. 3531–3573. Available at: https://doi.org/10.5194/tc-16-3531-2022.